3.2.1. Extraocular Retinal Prosthesis

The extraocular retinal prosthesis, which stimulates the visual cortex or optic nerve electrically, can be applied to patients with no retinal cells. This means that these methods can be applied to any disease, including RP and AMD. In the case in which the visual cortex is stimulated, the stimulator is implanted in the surface of the visual cortex by opening a scull. This method has been developed by the Dobelle Institute over a long period of time and has been successfully applied in some patients [28]. The method of stimulating the optic nerve involves covering the optic nerve with a cuff-type electrode to stimulate the nerve [27]. The cuff-type electrodes are illustrated in [29]. Both of these methods require difficult surgical operations because the surgical sites are related to the nervous system or the brain. These methods have only been performed in limited human trials. In addition, these methods must deal with retinotopy, which is the spatial correspondence between the retinal image and the recognition image in the brain. It is difficult to determine the correspondence between the input image and the electrode site on the visual cortex.

3.2.2. Intraocular retinal prosthesis

Stimulation of retinal cells involves an easier surgical procedure and is possibly less affected by retinotopy because the stimulation points are located near the retina. As mentioned previously, this method is classified into three types according to the stimulator implantation site: epi-retinal stimulation [18-21], sub-retinal stimulation [22-24], and STS [25,26]. Figure 6 illustrates these three types of retinal implantation. In these methods, the power supply and stimulus pattern data generated from input image data are transmitted wirelessly by electromagnetic coupling of the primary coil, which is placed outside the body, and the secondary coil, which is placed inside the body, as shown in Figure 7 [3].

Figure 6. Intraocular retinal prosthesis.

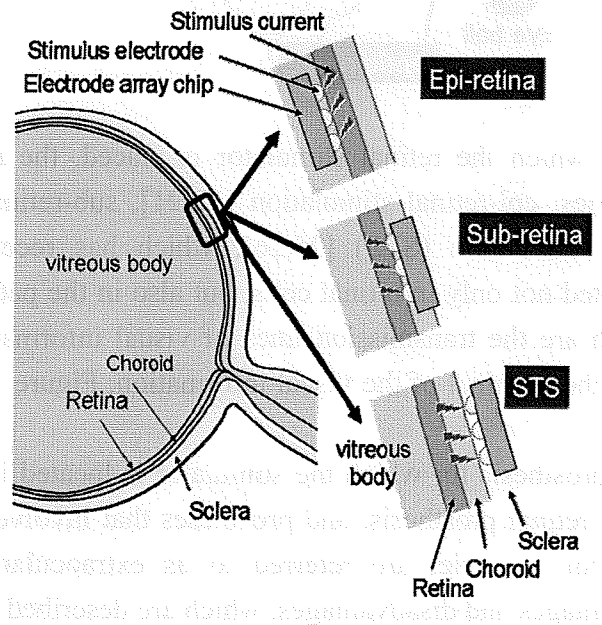

These wireless transmission technologies have been established for use in the artificial cochlear system [30]. In Figure 7, the secondary coil is implanted in the lens, but in some cases, it is implanted near the backside of the ear, as in the case of an artificial cochlear system.

Figure 7. Typical configuration of an intraocular retinal prosthesis system (adapted from [3] © 2009 IEEE).

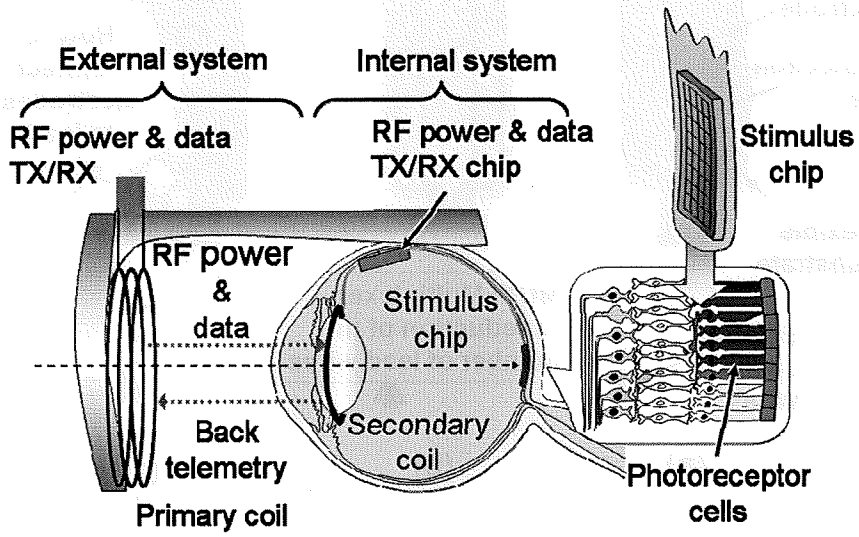

4. Retinal Stimulator Based On CMOS Technology

4.1. Realization of a Large Number of Stimulus Electrodes in a Retinal Stimulator

Several types of intraocular retinal prosthesis developed for use by blind patients have been reported [18-24], although, thus far, with the exception of [22], these prostheses have incorporated only small numbers of electrodes. In order to realize better vision through a retinal prosthesis, over 1,000 electrodes would be preferable. When increasing the number of electrodes, we are faced with problems associated with interconnection between electrodes and external lead wires with good mechanical flexibility. Specifically, the stimulator must be bent to match the curvature of the eyeball.

Figure 8 shows the methods used to realize a stimulus electrode array [4]. A direct connecting method, which is commonly used in retinal prosthesis devices, is shown in Figure 8(a), where each electrode is directly connected by a lead wire. A more sophisticated method is shown in Figure 8(b). In this method, a multiplexer is used to reduce the number of external lead wires. When further increasing the number of electrodes in Figure 8(b), it becomes difficult to connect electrodes to the multiplexer, simply as a result on the increased amount of wiring, as shown in Figure 8(c).

It is a good idea to introduce a CMOS-based chip in the stimulator because scanning circuits (scanner) can be integrated in order to reduce the amount of wiring, as shown in Figure 9(a). Random access can be implemented using decoder circuits instead of scanners. However, it is difficult to use a CMOS chip in a retinal stimulator device, because, for implantation, the CMOS-based stimulator should be thin and flexible in order to fit the eye and to avoid damaging tissue. However, silicon is rigid, and thinning of the CMOS chip increases the risk of breakage.

Figure 8. Problem of a large number of electrodes. (a) Direct wiring. (b) Embedding with MUX. (c) Large number of electrodes (adapted from [4]). MUX can reduce the number of external lead wires but not reduce the number of wires from electrodes to MUX.

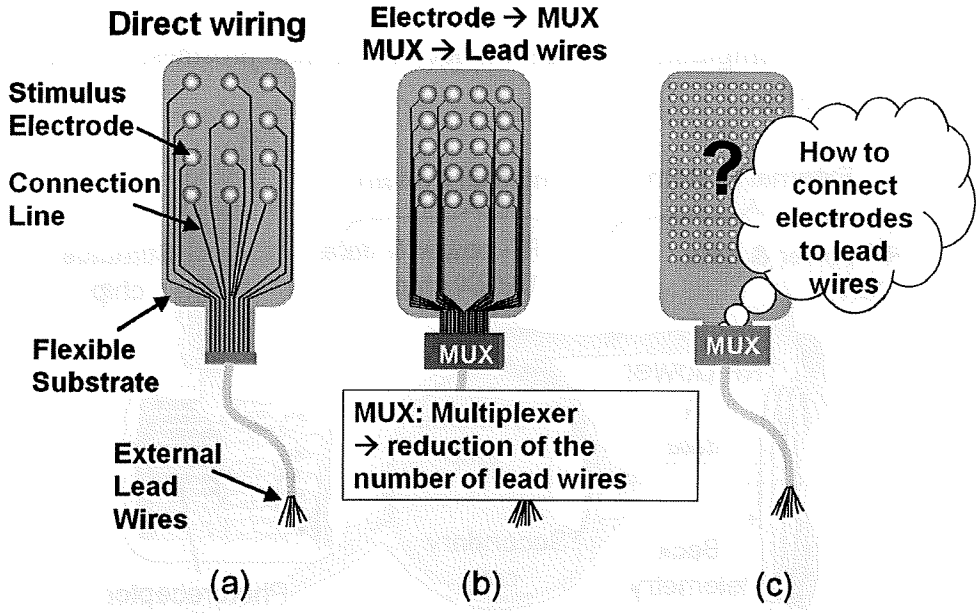

To solve this problem, we have already developed a new type of smart stimulator that consists of a number of CMOS-based microchips distributed on a flexible substrate, as shown in Figure 9(b) [1,2,4,5]. As shown in Figure 9(c), each microchip incorporates several stimulus electrodes, which can be externally controlled to turn on and off through an external control circuit. In addition to solving the interconnections issue, CMOS-based stimulators offer several advantages, such as signal processing. To allow flexibility, we place several microchips on a substrate in a distributed manner.

Figure 9. Realization of a large number of electrodes using CMOS technology. (a) CMOS chip. (b) Multiple microchip architecture. (c) Schematic diagram of the microchip (adapted from [4]).

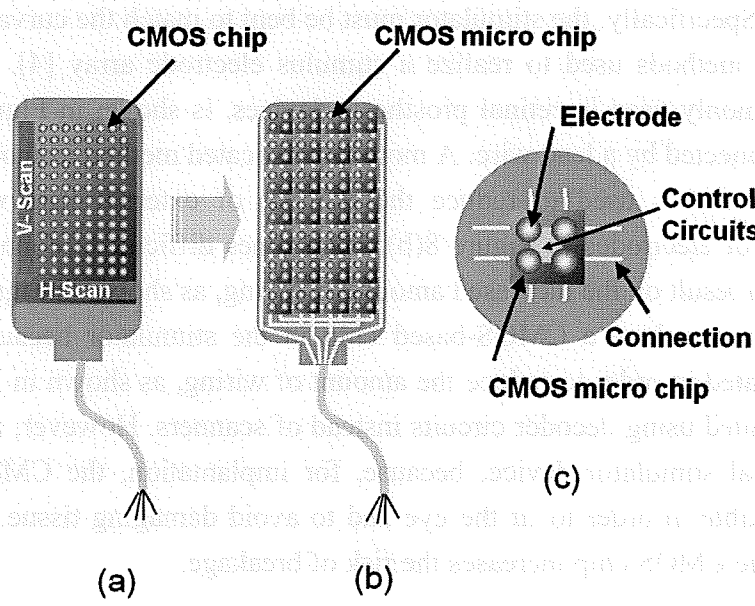

The substrate of the stimulator must have both mechanical flexibility and biocompatibility. Among several substrate materials, polymer materials such as polyimide, silicone and parylene are used to meet this requirement [31]. These features protect living tissues from the implanted stimulator, On the other hand, water-resistance is also required for the substrate feature to protect it from the biological environment, Parylene has good water resistant properties, while the others are not completely impervious to water penetration. Since parylene layers are hard to adhere to each other, making it difficult to sandwich metal wire lines in between, parylene is used to cover other substrate materials such as polyimide to protect the substrate from water.

4.2. Multiple Microchip Architecture for a Flexible Retinal Stimulator with a Large Number of Electrodes

4.2.1. Device design

We have proposed a new structure to realize an array having a large number of electrodes with better extendibility and better sealing characteristics in a biological environment, as compared with the previously proposed stimulator, as shown in Figure 10. This stimulator has been developed primarily for STS, which has been developed recently [25,26], and applied to blind patients. This stimulator can also be applied to other methods, such as sub-retinal stimulation. There are, however, numerous technical challenges that must be overcome when applying CMOS-based stimulators to retinal prostheses, as previously described in Section 2. Next, the device design of the microchip is described.

Figure 10. Multiple microchip architecture for a flexible retinal stimulator having a large number of stimulus electrodes.

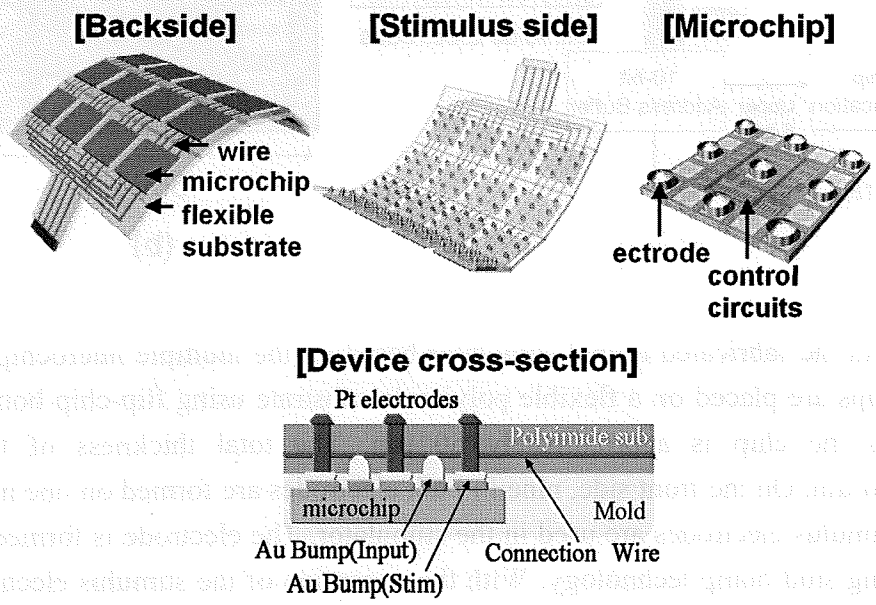

The microchip architecture has nine stimulation pads and four input lines, including the power supply lines. A block diagram of the chip is shown in Figure 11(a) [4]. Each stimulation pad is assigned a unique four-bit address that can selectively activate one of the nine electrodes on the

microchip. The four input lines are VDD, GND, CTLR, and STIM. The VDD and GND lines are used for the power supply (VDD = 5 V), and control and stimulation can be achieved with only two lines, namely, CTLR and STIM. Each of the stimulation electrodes can be selected with the number of the pulses applied on the CTLR line. This is achieved by the microchip counting the pulses applied on the CTLR line using a 10-bit address buffer. As shown in Figure 11(a), the lower four bits of the address buffer are used for electrode selection, and the upper six bits are used for chip identification. The stimulation current is provided from outside the chip and is fed into the STIM terminal.

One of the stimulation electrodes is selected depending on the value in the lower four bits of the address buffer. The six-bit address space for microchips facilitates the control of an arbitrary number of microchips (up to 64) using only one set of input lines. Consequently, the multi-chip stimulation device platform can configure a 64-chip device with 576 stimulation electrodes. In order to ensure flexibility, the microchip array is assembled at a pitch of 1,000 to 1,200 μm. The microchips are diced from a mother chip, which is fabricated using 0.35 μm standard CMOS technology. The mother chip contains 16 microchips. Figure 11(b) shows microphotographs of a mother chip and a microchip measuring 600 μm × 600 μm.

Figure 11. Block diagram (a) and microphotograph (b) of the microchip (adapted from [4]).

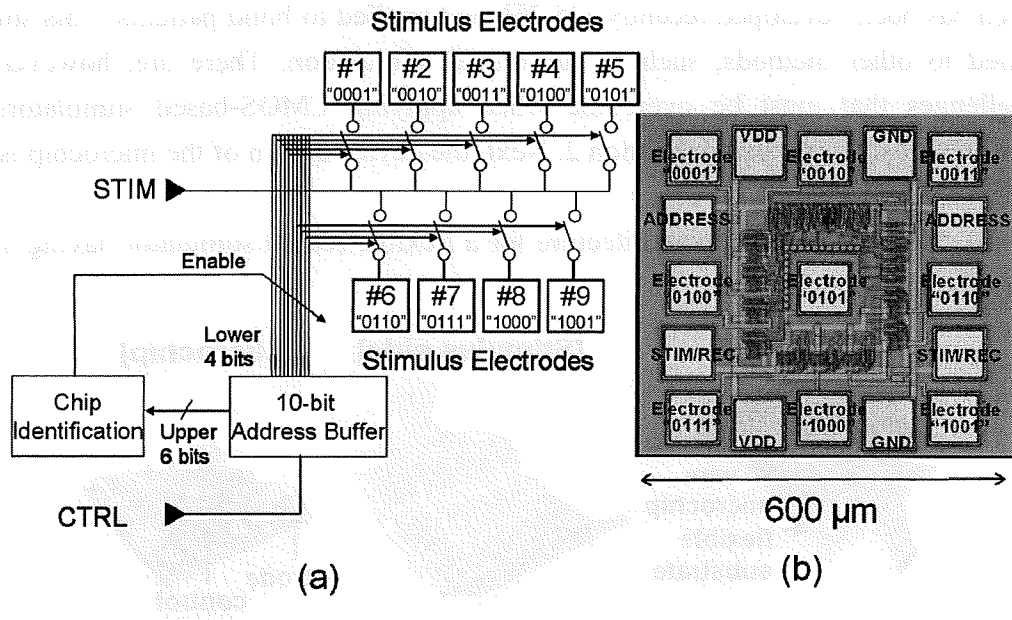

Figure 12 shows the fabricated retinal stimulator based on the multiple microchip architecture [5]. The four microchips are placed on a flexible polyimide substrate using flip-chip bonding technology. The thickness of the chip is approximately 50 μm. The total thickness of the stimulator is approximately 200 μm. On the front side, nine Pt bulk electrodes are formed on one microchip, so that, in this case, 36 stimulus electrodes are used in the stimulator. The electrode is formed on an Al pad of the microchip using stud bump technology. With the exception of the stimulus electrodes, the surface of the stimulator is covered with epoxy resin or palylene. As shown in Figure 12, the fabricated stimulator can be bent easily, and the radius in this case is approximately the same as that of the rabbit eyeball, *i.e.*, 1.7 mm.

Figure 12. Fabricated retinal stimulator based on the multiple microchip architecture (adapted from [5]).

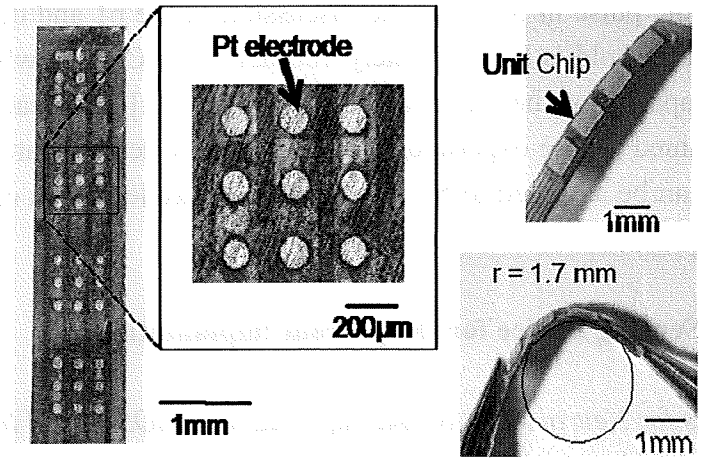

4.2.2. *In vivo* operation

We conducted an *in vivo* experiment in which we implanted the fabricated stimulator into the scleral pocket of a rabbit eye using an operation procedure described in reference [26]. The rabbit was anesthetized. The recording electrode used to measure the electrical evoked potential (EEP) was a stainless-steel screw. The electrode was screwed into the skull at the area of the visual cortex so that the tip touched the dura mater. The reference electrode was screwed into the bregma. The stimulator was inserted into a pocket formed in sclera. A return electrode was inserted into the vitreous cavity. Monophasic 0.5-ms-duration pulses with anodic polarity were used to elicit the EEPs. The pulse used was a single anodic pulse. The responses to 20 to 30 stimuli were averaged for EEP.

Figure 13. EEP signals obtained in an *in vivo* experiment using the implanted retinal stimulator.

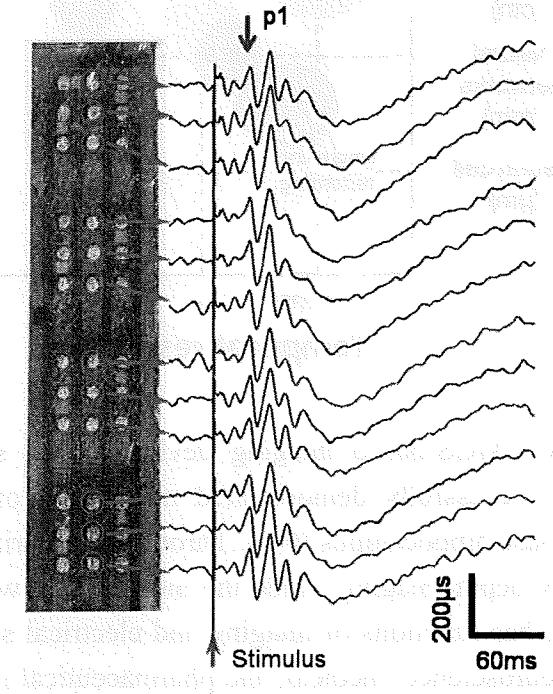

Figure 13 shows the experimental results for the EEPs, where "p1" was concluded to be the EEP signal from the ganglion cells because of the latency of the signal. An anodic pulse was found to be more excited than a cathodic pulse in STS and the discussion of the p1 and other peaks are appeared in [26]. Based on p1, the threshold is approximately 100 μA (<1 mC/cm^2), which is considered to be adequate for the charge capacity of the electrode (1–4 mC/cm^2 [31]). For each stimulus electrode, a clear EEP signal was obtained. These experimental results clearly demonstrate that any one electrode among the 36 electrodes can be assigned to be the stimulus electrode, which can be used to stimulate retinal cells.

5. *In vivo* CMOS Image Sensing Device for Deep Brain Implantation

5.1. Measurement Methods for Neural Activity and Implantable CMOS-Based Imaging Device

There is significant demand for devices that can monitor *in vivo* neural activity in the deep brain of small animals, such as the mouse, in real time [32-34]. This requires that the device be able to detect activities with a spatial resolution of less than 1 mm and a temporal resolution of less than 1 sec. However, this is difficult for current measurement methods, such as functional magnetic resonance imaging (fMRI), positron emission tomography (PET), and near infrared spectroscopy (NIRS) to meet both of these requirements, as shown in Figure 14 [31].

Figure 14. Spatio-temporal map of measurement technologies for neural activity (adapted from [31]).

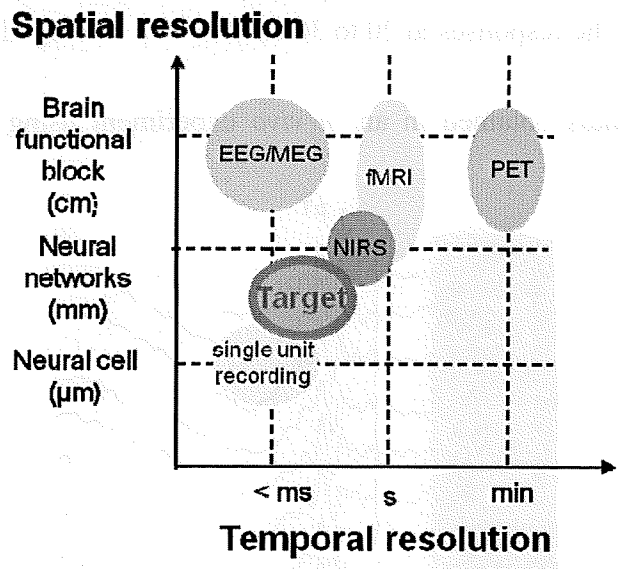

We have developed a new CMOS-based imaging device with a sub-mm, sub-second spatio-temporal resolution and have successfully demonstrated monitoring of the time course of serine protease activities inside the mouse hippocampus [6-9]. Through appropriate packaging, the developed device can be used for arbitrary depth imaging inside the mouse brain with minimal impact on brain function. The developed device has functions of imaging and electrical stimulation, which will result in a new bio-imaging tool for neuroscience, medical, and pharmaceutical research.

We have demonstrated the effectiveness of the device for monitoring the neural activity *in vivo* when the mouse is immobilized [6]. The device is a CMOS-based image sensing chip embedded with electrodes. The chip and excitation UV-LED are placed on a flexible polyimide substrate, as shown in Figure 15. Recently, we have demonstrated the ability to monitor neural activity in the "freely-moving" mouse. In the following section, we briefly summarize the specifications of the developed device. We then show the experimental results of monitoring neural activity in the mouse brain. Finally, a new device that is designed to ensure sufficient fixation in the brain for a freely-moving mouse is presented.

Figure 15. Schematic diagram of an implantable CMOS-based imaging device (adapted from [7]).

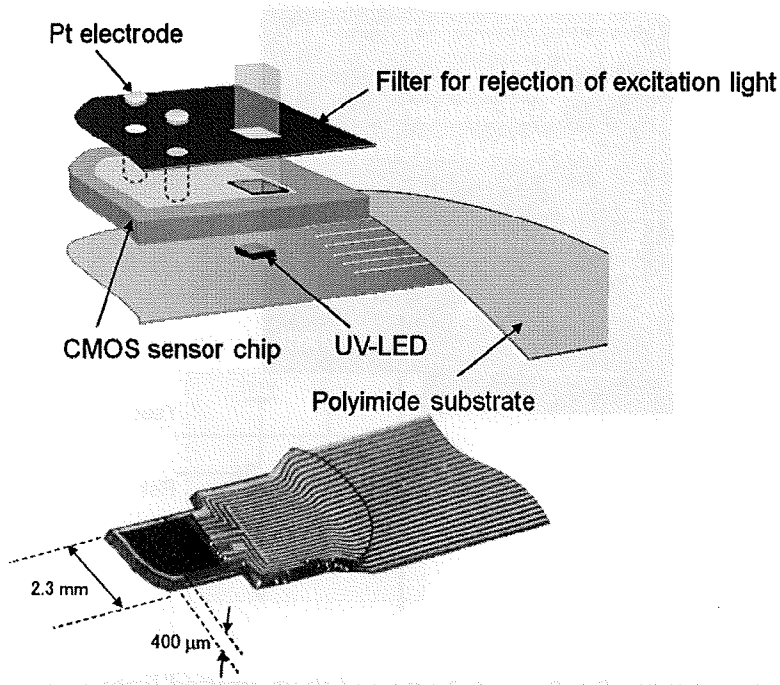

5.2. Device Structure and Specifications

The CMOS chip is based on a CMOS image sensor fabricated using standard 0.35 μm CMOS technology. The pixel structure is a three-transistor type active pixel sensor (APS) with a parasitic photodiode composed of n-wells and p-substrate junctions. The specifications of the image sensor are summarized in Table 1.

Figure 15 shows a photomicrograph of the sensor chip [7]. The chip has four stimulus electrode pads (white squares in the figure) and 30 through-holes for excitation light on the surface next to the image sensor pixels.

Table 1. Specifications of the implantable CMOS imaging chip.

Technology	**0.35 μm 2-poly 4-metal standard CMOS**
Power supply voltage	3.3 V
Chip size	2 mm × 2.24 mm
Pixel type	3-Transistor APS
Pixel number	216 × 144
Pixel size	7.5 μm × 7.5 μm
Photodiode	parasitic n-well/p-substrate diode

Figure 16. Photomicrograph of the chip. The inset shows the pixel circuit (adapted from [7]).

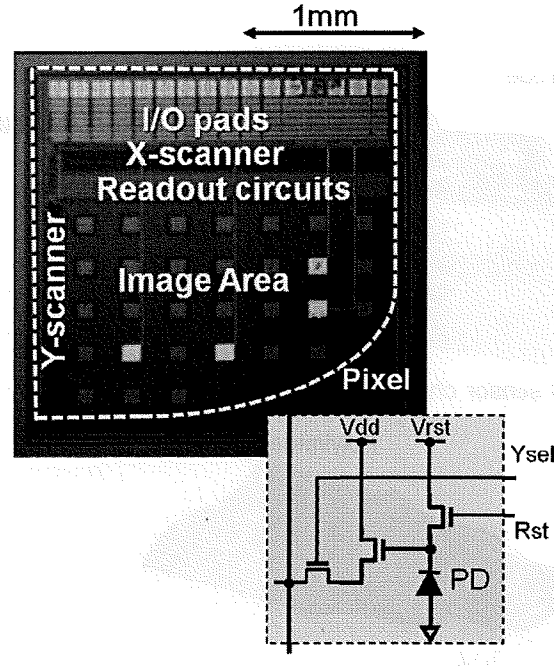

UV-LEDs can be placed under the through-holes and their emitted light is transmitted through these holes and excited tissues. In some experiments, the UV-LED has been placed next to the chip. The Pt bump can be formed on the electrode pad as a bulk stimulus electrode, as described in Reference [8]. The image sensor surface is coated with a blue filter to suppress the excitation light impinging on the image plane, as mentioned in reference [8]. The total width of the sensor device is approximately 3 mm. The shape of the top of the device is round in order to minimize damage to the tissue during insertion into the brain. The sensor chip and UV-LED are mounted on a polyimide substrate. In the substrate, metal wires are routed from the chip and the UV-LED to an external controller and a power supply. The entire device is covered with an epoxy resin in order to protect the device from the water environment.

5.3. In Vivo Experiment Using the Implantable CMOS Imaging Sensor Device

In order to demonstrate the device for functional imaging of the mouse brain, an experiment that involves imaging serine protease activity in the hippocampus was designed and performed. Serine protease is related to memory and learning in the hippocampus. Kainic acid (KA) is a well-known

chemical stimulant that can induce the extracellular release of serine protease. In order to detect the activity of serine protease in the hippocampus, synthetic substrate MCA was used. MCA is cleaved by serine protease. The substrate is hydrolyzed due to the presence of the protease, which acts as a catalyst. Once hydrolyzed, the released aromatic amine fluorophore, AMC, fluoresces intensely with a peak wavelength at 470 nm when excited by a UV light source. This fluorescence is used as an indicator of serine protease activity. This process is illustrated in Figure 17.

Figure 17. Measurement method of detecting neural activity thorough fluorescence.

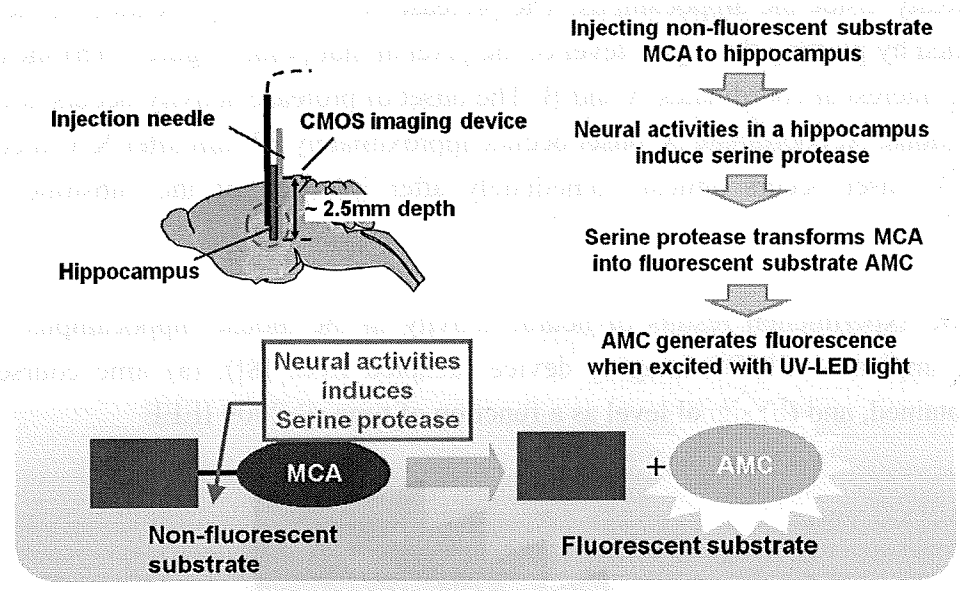

Figure 18. Experimental setup of measuring neural activity in the mouse hippocampus.

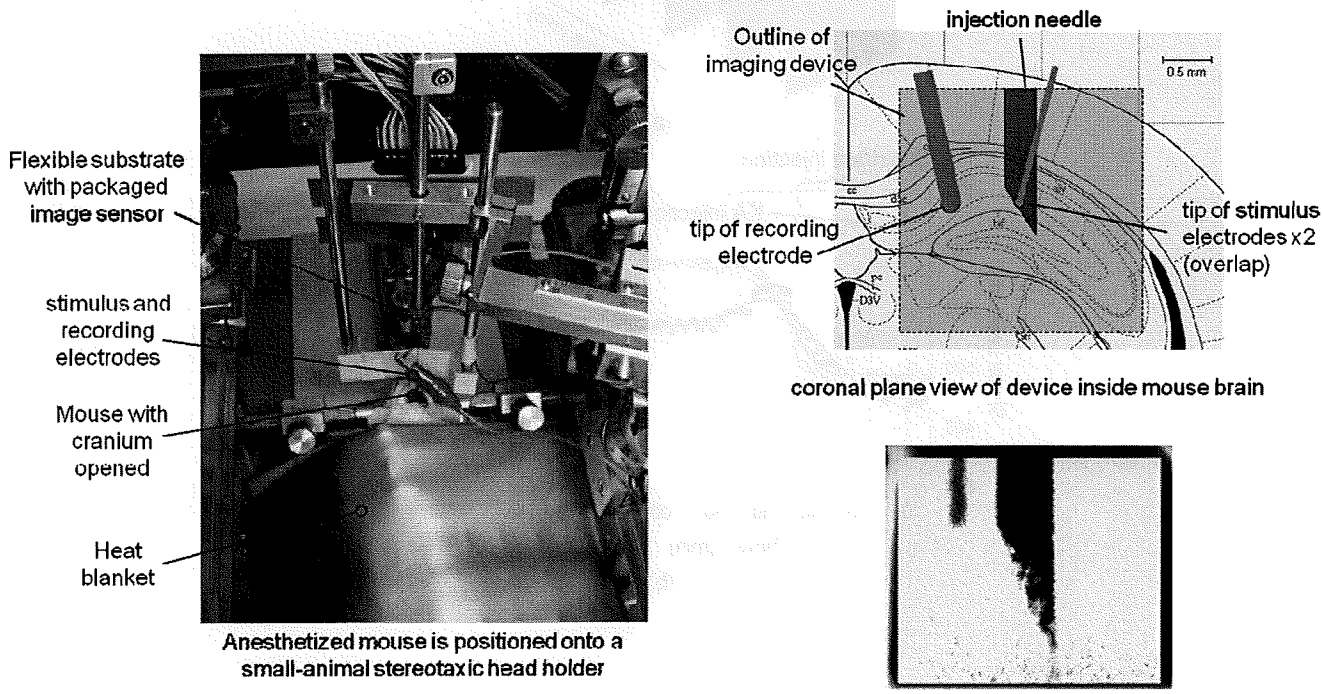

It is noted that our sensor can detect fluorescence through diffused light. We have already confirmed that the device can detect the diffused light in the depth of about 500 μm [35].

The preparation of the mouse for the surgical procedure and imaging has been reported previously [9]. The packaged device with the attached needle was used in the experiment. Figure 18 shows the position of the device inside the mouse brain.

This substrate solution was used to maximize the available fluorescence signal inside the brain. Fifteen minutes before the substrate pump started, KA was injected intraperitoneally. Figure 19 shows the images captured by the device during the experiment [8]. The fluorescence pattern appears to change dynamically inside the hippocampus. The protease activity at any location in the hippocampus can be determined by plotting the signal level of the pixel at that point. Figure 19(b) shows the activity of two points of interest at coordinates A and B. The onset of protease activity occurs at different times at different locations. At coordinate A, onset occurs approximately 33 min after KA injection, whereas at coordinate B, onset occurs almost immediately after injection of the substrate, 15 min after KA injection.

Figure 19. Experimental results of neural activity in the mouse hippocampus obtained using the implanted CMOS imaging device (adapted from [8]). (a) time course of the images obtained, and (b) signal level as a function of time. © 2009 IEEE

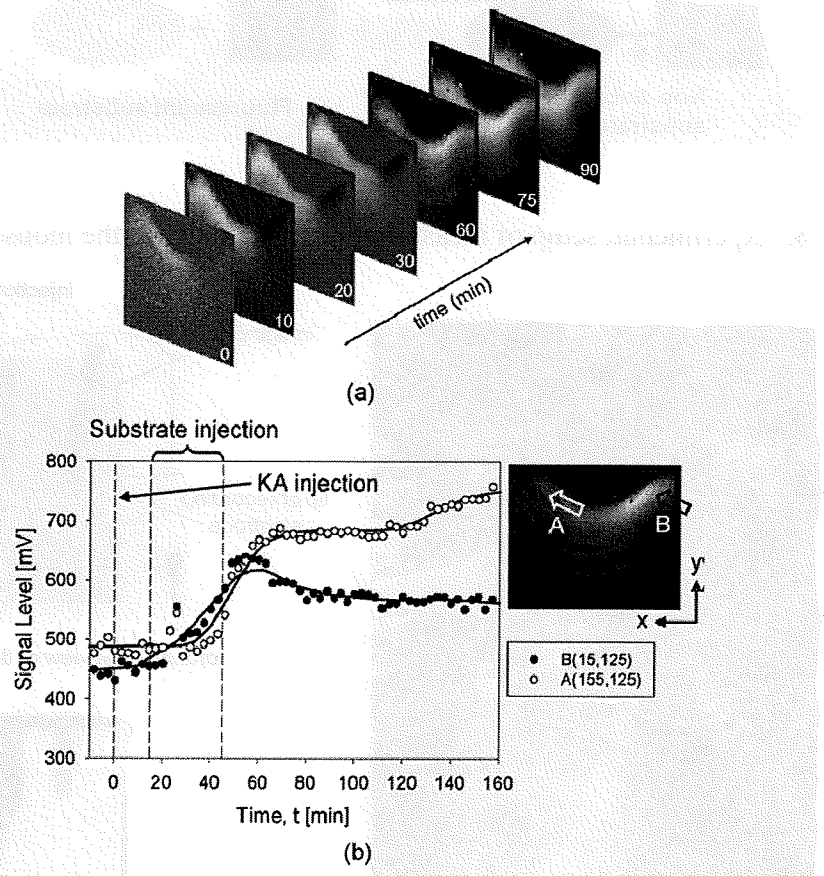

5.4. Measurement of Neural Activity in the Brain of the Freely-Moving Mouse

In order to detect neural activity in the deep brain of the freely-moving mouse, it is necessary to more effectively stabilize the sensor. We are currently developing a new sensor chip, which is shown in Figure 20 [36]. The new sensor is narrower than the previous sensor, which enables the new sensor to be more tightly fixed to the tissue. The fabricated device is also shown in Figure 20. The width of the device is about 2 mm, which is much thinner than that of the previous device. In addition, we are now planning to reduce the number of input/output (I/O) ports in the new sensor to four: the input clock, the output signal, VDD, and GND. The bias voltage can be adjusted after fabrication by trimming the resistor array embedded in the chip. The four bias voltage circuits are used in the chip. The chip specifications are the same as in previous chips, except for the width of the chip and the number of I/Os.

Figure 20. Microphotograph of the sensor chip and the fabricated device implanted into the brain of the freely moving mouse (adapted from [36]). The surface is coated with green filter for GFP (green fluorescence protein). Two LEDs for excitation of GFP are placed on the side of the chip.

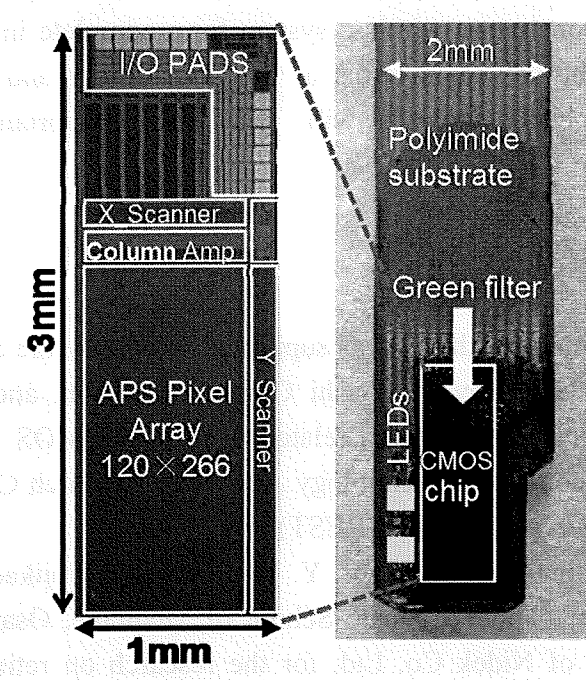

6. Conclusions

Implantable CMOS devices are very useful for biomedical applications but there are still a lot of issues to be considered. In this review, we mention two examples of the implantable CMOS devices for biomedical applications; one is s retinal prosthesis and the other is an *in vivo* brain implantable CMOS imaging device.

A retinal stimulator based on multiple microchip based architecture for a large number of stimulus electrodes in STS is described. Better extendibility and reliability are demonstrated, as compared with

the previously proposed stimulators. Using the stimulator implanted in a rabbit, the EEP signal has been observed with a threshold of 100 μA.

The next step in our retinal prosthesis device is to ensure durability and biocompatibility in long term operation inside living tissue. One of the most difficult issues is a package for a Si microchip. Parylene is a good candidate for the package, but for the long term, such as ten years, it is not unknown whether parylene will maintain its the water-resistant characteristics or not. A ceramic hermetic case is effective for water-resistance, but it has a large volume for a microchip. Deposited film of metal is also effective but it is difficult to deposit metal film with no pinholes. If pinholes exist, water can penetrate into the chip. The implantable CMOS image sensing device in the mouse brain is introduced for monitoring the neural activity in the deep brain of a mouse. This demonstrates the effectiveness of the proposed device for use in brain science. The next generation sensor is also shown for freely-moving mouse. The previously-developed device shown in Figure 16 has been demonstrated to operate properly over two weeks. In such short term operation, the UV-LED does not affect tissues, but we need to investigate the effects over longer terms. In addition, we need to exectute the similar test for the newly-developed device shown in Figure 20.

The next step in the implantable CMOS image sensing device is to improve the resolution of the sensor. Bulky optics is not suitable for the implantable device. Microoptics is one of the candidates. The other requirement is to construct a wireless system for a complete implantable device. Although there are a lot of issues to be solved in terms of biocompatibility and durability for a long term operation, implantable CMOS devices will play an important role for the future biomedical applications.

Acknowledgements

The research related to retinal prostheses was supported in part by the Strategic Research Program for Brain Sciences, MEXT, Japan, by the Asahi Glass Foundation, and by a Health and Labour Sciences Research Grant, Japan. The research related to *in vivo* CMOS image sensing devices was supported in part by the Semiconductor Technology Academic Research Center (STARC), and by the Japan Science and Technology Agency (JST-CREST).

The authors would like to thank the late Prof. Y. Tano, Prof. T. Fujikado, Prof. M. Kamei, Dr. K. Nishida, and Dr. Y. Kitaguchi of the Graduate School of Medicine, Osaka University, and Mr. M. Ozawa and Dr. Y. Terasawa of Nidek Co. Ltd. for the research on retinal prosthesis. The authors would also like to thank Prof. S. Shiosaka, Prof. H. Tamura, Prof. Y. Ishikawa, and Dr. Y. Hatanaka for the research on *in vivo* CMOS imaging devices. The present report was also supported by the VLSI Design and Education Center (VDEC), University of Tokyo, in collaboration with Cadence Design Systems, Inc.

References

1. Tokuda, T.; Pan, Y.-L.; Uehara, A.; Kagawa, K.; Nunoshita, M.; Ohta, J. Flexible and extendible neural interface device based on cooperative multi-chip CMOS LSI architecture. *Sens. Actuat. A* **2005**, *122*, 88-98.
2. Ohta, J.; Tokuda, T.; Kagawa, K.; Furumiya, T.; Uehara, A.; Terasawa, Y.; Ozawa, M.; Fujikado, T.; Tano, Y. Silicon LSI-Based Smart Stimulators for Retinal Prosthesis. *IEEE Eng. Med. Biol. Mag.* **2006**, *25*, 47-59.
3. Ng, D.C.; Furumiya, T.; Yasuoka, K.; Uehara, A.; Kagawa, K.; Tokuda, T.; Nunoshita, M.; Ohta, J. Pulse frequency modulation based CMOS image sensor for subretinal stimulation. *IEEE Trans. Circ. Syst. II* **2006**, *53*, 487-491.
4. Ohta, J.; Tokuda, T.; Kagawa, K.; Sugitani, S.; Taniyama, M.; Uehara, A.; Terasawa, Y.; Nakauchi, K.; Fujikado, T.; Tano, Y. Laboratory investigation of microelectronics-based stimulators for large-scale suprachroidal transretinal stimulation (STS). *J. Neural Eng.* **2007**, *4*, S85-S91.
5. Tokuda, T.; Asano, R.; Sugitani, S.; Taniyama, M.; Terasawa, Y.; Nunoshita, M.; Nakauchi, K.; Fujikado, T.; Tano, Y.; Ohta, J. Retinal stimulation on rabbit using CMOS-based multi-chip flexible stimulator toward retinal prosthesis. *Jpn. J. Appl. Phys.* **2008**, *47*, 3220-3225.
6. Ng, D.C.; Tamura, H.; Tokuda, T.; Yamamoto, A.; Matsuo, M.; Nunoshita, M.; Ishikawa, Y.; Shiosaka, S.; Ohta, J. Real time in vivo imaging and measurement of serine protease activity in the mouse hippocampus using a dedicated CMOS imaging device. *J. Neurosci. Meth.* **2006**, *156*, 2006.
7. Ng, D.C.; Tamura, H.; Mizuno, T.; Tokuda, T.; Nunoshita, M.; Ishikawa, Y.; Shiosaka, S.; Ohta, J. An implantable and fully-integrated complementary metal-oxide semiconductor device for in vivo neural imaging and electrical interfacing with the mouse hippocampus. *Sens. Actuat. A* **2008**, *145-146*, 176-186.
8. Ng, D.C.; Nakagawa, T.; Mizuno, T.; Tokuda, T.; Nunoshita, M.; Tamura, H.; Ishikawa, Y.; Shiosaka, S.; Ohta, J. Integrated in vivo neural imaging and interface CMOS devices: design; packaging; and implementation. *IEEE Sens. J.* **2008**, *8*, 121-130.
9. Tamura, H.; Ng, D.C.; Tokuda, T.; Naoki, T.; Nakagawa, T.; Mizuno, T.; Hatanaka, Y.; Ishikawa, Y.; Ohta, J.; Shiosaka, S. One-chip sensing device (Biomedical photonic LSI) enabled to assess hippocampal steep and gradual up-regulated proteolytic activities. *J. Neurosci. Meth.* **2008**, *173*, 114-120.
10. Roham, M.; Garris, P.; Mohseni, P. A wireless multichannel IC for time-share chemical and electrical neural recording. In *Proceedings of IEEE International Solid State Circuits Conference*, San Francisco, CA, USA, 2009; pp. 430-431.
11. Agnew, W.F.; McCreery, D.B.; Yuen, T.G.H.; Bullara, L.A. Effects of Prolonged Electrical Stimulation of the Central Nervous System. In *Neural Prostheses*; Prentice Hall: Englewood Cliffs, NJ, USA, 1990.
12. Robblee, L.S.; Rose, T.L. Electrochemical Guidelines for Selection of Protocols and Electrode Materials for Neural Stimulation. In *Neural Prostheses*; Prentice Hall: Englewood Cliffs, NJ, USA, 1990.

13. McCreery, D.B.; Agnew, W.F. Mechanics of Stimulation-Induced Neural Damage and Their Relation to Guidelines for Safe Stimulation. In *Neural Prostheses*; Prentice Hall: Englewood Cliffs, NJ, USA, 1990.
14. Wandell, B.A. *Foundations of Vision*; Sinauer Associates Inc.: Sunderland, MA, USA, **1995**.
15. Research Report by Ministry of Health, Labour, and Welfare of Japan, 2005.
16. Santos, A.; Humayun, M.S.; de Juan, E.; Greenburg, R.J.; Marsh, M.J.; Klock, I.B.; Milam, A.H. Preservation of the inner retina in retinitis pigmentosa; a morphometric analysis. *Arch. Ophthalmol.* **1996**, *114*, 40-46.
17. Humayun, M.S.; Prince, M.; de Juan, E.; Barron, Y.; Moskowitz, M.; Klock, I.B.; Milam, A.H. Morphometric analysis of the extramacular retina from postmorten eyes with retinitis pigmentosa. *Invest. Ophthalmol Vis. Sci.* **1999** *40*, 143-148.
18. Liu, W.; Humayun, M.S. Retinal Prosthesis. *IEEE Int. Solid-State Cric. Conf.—Dig. Tech. Papers* **2004**, pp. 218-219.
19. Humayun, M.S.; Weiland, J.D.; Fujii, G.Y.; Greenberg, R.; Williamson, R.; Little, J.; Mech, B.; Cimmarusti, V.; van Boemel, G.; Dagnelie, G.; de Juan, E., Jr. Visual perception in a blind subject with a chronic microelectronic retinal prosthesis. *Vision Res.* **2003**, *43*, 2573-2581.
20. Rizzo, J.F., III; Wyatt, J.; Loewenstein, J.; Kelly, S.; Shire, D. Methods and perceptual thresholds for short-term electrical stimulation of human retina with microelectrode Arrays. *Invest. Ophthalmol. Vis. Sci.* **2003**, *44*, 5355-5361.
21. Hornig, R.; Laube, T.; Walter, P.; Velikay-Parel, M.; Bornfeld, N.; Feucht, M.; Akguel, H.; Rössler, G.; Alteheld, N.; Notarp, D.L.; Wyatt, J.; Richard, G. A method and technical equipment for an acute human trial to evaluate retinal implant technology. *J. Neural. Eng.* **2005**, *2*, S129-S134.
22. Chow, A.Y.; Chow, V.Y.; Packo, K.; Pollack, J.; Peyman, G.; Schuchard, R. The artificial silicon retina microchip for the treatment of vision loss from retinitis pigmentosa. *Arch. Ophthalmol.* **2004**, *122*, 460-469.
23. Zrenner, E. Will retinal implants restore vision? *Science* **2002**, *295*, 1022-1025.
24. Sachs, H.G.; Schanze, T.; Wilms, M.; Rentzos, A.; Brunner, U.; Gekeler, F.; Hesse, L. Subretinal implantation and testing of polyimide film electrodes in cats. *Graefe's Arch. Clin. Exp. Ophthalmol.* **2005**, *243*, 464-468.
25. Kanda, H.; Morimoto, T.; Fujikado, T.; Tano, Y.; Fukuda, Y.; Sawai, H. Electrophysiological studies of the feasibility of suprachoroidal-transretinal stimulation for artificial vision in normal and RCS rats. *Invest. Ophthal. Vis. Sci.* **2004**, *45*, 560-566.
26. Nakauchi, K.; Fujikado, T.; Kanda, H.; Morimoto, T.; Choi, J.S.; Ikuno, Y.; Sakaguchi, H.; Kamei, M.; Ohji, M.; Yagi, T.; Nishimura, S.; Sawai, H.; Fukuda, Y.; Tano, Y. Transretinal electrical stimulation by an intrascleral multichannel electrode array in rabbit eyes. *Graefe's Arch. Clin. Exp. Ophthalmol.* **2005**, *243*, 169-174.
27. Veraart, C.; Wanet-Defalque, M.C.; Genard, B.; Vanlierde, A.; Delbeke, J. Pattern recognition with the optica nerve visual prosthesis. *Artif. Organs* **2003**, *11*, 996-1004.
28. Dobelle, W.H. Artificial vision for the blind by connecting a television camera to the visual cortex. *ASAIO J.* **2000**, *46*, 3-9.

29. Naples, G.G.; Mortimer, J.T.; Scheiner, A.; Sweeney, J.D. A spiral nerve cuff electrode for peripheral nerve stimulation. *IEEE Trans. Biomedical Eng.* ***1998***, *35*, 905-916.
30. Seligman, P.M.; Shepherd, R.K. Cochlear Implants. In *Neuroprothetics*; Kenneth, W.H., Dhilon, G.S., Eds.; World Scientific Publishing Co. Pte. Ltd.: Singapore, 2004.
31. Weiland, J.D.; Liu, W.; Humayun, M.S. Retinal prosthesis. *Annu. Rev. Biomed. Eng.* **2005**, *7*, 361-401.
32. Mazziota, J.C. Time and Space. In *Brain Mapping the Methods*, 2nd ed.; Toga, A.W., Mazziota, J.C., Eds.; Academic Press: New York, NY, USA, 2002; pp. 33-44.
33. Helmchen, F.; Fee, M.S.; Tank, D.W.; Denk, W. A miniature head-mounted neurotechnique two-photon microscope: high resolution brain imaging in freely moving animals. *Neuron* **2001**, *31*, 903-912.
34. Berger, T.W.; Baudry, M.; Brinton, R.D.; Liaw, J.-S.; Marmarelis, V.Z.; Park, A.Y.; Sheu, B.J.; Tanguay, A.R., Jr. Brain-implantable biomimetic electronics as the next era in neuralprosthetics. *Proc. IEEE* **2001**, *89*, 993-1012.
35. Ng, D.C.; Tokuda, T.; Yamamoto, A.: Matsuo, M.: Nunoshita, M.; Tamura, H.; Ishikawa, Y.; Shiosaka, S.; Ohta, J. On-chip biofluorescence imaging inside a brain tissue phantom using a CMOS image sensor for in vivo brain imaging verification, *Sens. Actuat. B* **2006**, *119*, 262-274.
36. Tagawa, A.; Higuchi, A.; Sugiyama, T.; Sasagawa, K.; Tokuda, T.; Tamura, H.; Hatanaka, Y.; Shiosaka, S.; Ohta, J. Development of complementary metal oxide semiconductor imaging devices for detecting green fluorescent protein in the deep brain of a freely moving mouse. *Jpn. J. Appl. Phys.* **2009**, *48*, 04C195-1-5.

ELectronics EXpress

IEICE Electronics Express, Vol.5, No.15, 574–580

A visual prosthesis with 100 electrodes featuring wireless signals and wireless power transmission

Yasuo Terasawa[1,2a)], Akihiro Uehara[1,2], Eiji Yonezawa[1], Tohru Saitoh[1], Kenzo Shodo[1,2], Motoki Ozawa[1], Yasuo Tano[3], and Jun Ohta[2]

[1] *Vision Institute, Nidek Co.,Ltd*

73–1 Hama-cho, Gamagori, Aichi 443–0036, Japan

[2] *Materials Science, Nara Institute of Science and Technology,*

8916–5 Takayama-cho, Ikoma, Nara 630–0101, Japan

[3] *Department of Ophthalmology, Graduate School of Medicine, Osaka University,*

2–2 Yamadaoka, Suita, Osaka 565–0871, Japan

a) *yasuo_terasawa@nidek.co.jp*

Abstract: A visual prosthesis is an artificial sensory organ that transmits visual information to a blind person by electrically stimulating residual neurons in the visual nervous system. Such a system requires a large number of stimulating electrodes: It is technically difficult to connect a stimulator placed behind the ear to each of the stimulating electrodes over any significant distance with high reliability. We propose a visual prosthesis containing a multiplexer that is separately placed from the stimulator unit. The array of stimulating electrodes is connected to the stimulation unit through a multiplexer. The stimulating electrodes and multiplexer are placed onto the suprachoroidal space. The stimulation unit consists of a metal case and a coil and is implanted in the postauricular region of the cranium. The multiplexer and the stimulator unit are connected by a cable composed of six wires. Incorporating the multiplexer enables us to control of a large number of electrodes using a small number of conductors in the cable. We have developed a system with 100 electrodes which is powered and controlled wirelessly. Then we have confirmed that the proposed system functions successfully both in vitro and in vivo.

Keywords: visual prostheses, electrode, multiplexer

Classification: New functional devices and materials

References

[1] M. S. Humayun, J. D. Weiland, G. Y. Fujii, R. Greenberg, R. Williamson, J. Little, B. Mech, V. Cimmarusti, G. V. Boemel, G. Dagnelie, and E.

DOI: 10.1587/elex.5.574
Received June 23, 2008
Accepted July 10, 2008
Published August 10, 2008

de Juan Jr, "Visual perception in a blind subject with a chronic microelectronic retinal prosthesis," *Vis. Res.*, vol. 43, pp. 2573–2581, 2003.

[2] E. Zrenner, A. Stett, S. Weiss, R. B. Aramant, E. Guenther, K. Kohler, K.-D. Milliczek, M. J. Seiler, and H. Haemmerle, "Can subretinal microphotodiodes successfully replace degenerated photoreceptors?," *Vis. Res.*, vol. 39, pp. 2555–2567, 1999.

[3] G. Richard, R. Hornig, M. Keseru, and M. Feucht, "Chronic Epiretinal Chip Implant in Blind Patients with Retinitis Pigmentosa: Long-Term Clinical Results," *Invest. Ophthalmol. Vis. Sci.*, vol. 48, no. 5, p. S666, 2007.

[4] H. Kanda, T. Morimoto, T. Fujikado, Y. Tano, Y. Fukuda, and H. Sawai, "Electrophysiological Studies of the Feasibility of Suprachoroidal-Transretinal Stimulation for Artificial Vision in Normal and RCS Rats," *Invest. Ophthalmol. Vis. Sci.*, vol. 45, no. 2, pp. 560–566, 2004.

[5] M. S. Humayun, J. Hopkins, S. H. Greenwald, A. Horsager, A. Roy, K. H. McClure, G. Palmer, I. Fine, M. J. McMahon, and R. J. Greenberg, "Electrical Effects and Perceptual Performance Using a Chronically Implanted 16-Channel Epiretinal Prosthesis in Blind Subjects," *Invest. Ophthalmol. Vis. Sci.*, vol. 47, no. 5, p. S3212, 2006.

[6] M. J. McMahon, A. Caspi, J. D. Dorn, K. H. McClure, M. S. Humayun, and R. J. Greenberg, "Spatial Vision in Blind Subjects Implanted With the Second Sight Retinal Prosthesis," *Invest. Ophthalmol. Vis. Sci.*, vol. 48, no. 5, p. S4443, 2007.

[7] G. Dagnelie, D. Barnett, M. S. Humayun, and R. W. Thompson, Jr, "Paragraph Text Reading Using a Pixelized Prosthetic Vision Simulator: Parameter Dependence and Task Learning in Free-Viewing Conditions," *Invest. Ophthalmol. Vis. Sci.*, vol. 47, no. 3, pp. 1241–1250, 2006.

[8] J. Sommerhalder, E. Oueghlani, M. Bagnoud, U. Leonards, A. B. Safran, and M. Pelizzone, "Simulation of artificial vision: I. Eccentric reading of isolated words, and perceptual learning," *Vis. Res.*, vol. 43, pp. 269–283, 2003.

[9] J. Ohta, T. Tokuda, K. Kagawa, T. Furumiya, A. Uehara, Y. Terasawa, M. Ozawa, T. Fujikado, and Y. Tano, "Silicon LSI-based smart stimulators for retinal prosthesis," *IEEE Eng. Med. Biol. Mag.*, vol. 25, no. 5, pp. 45–59, 2006.

[10] Y. Terasawa, H. Tashiro, A. Uehara, T. Saitoh, M. Ozawa, T. Tokuda, and J. Ohta, "The development of a multichannel electrode array for retinal prostheses," *J. Artif. Organs.*, vol. 9, pp. 263–266, 2006.

[11] T. Stieglitz, H. Beutel, R. Keller, C. Blau, and J.-U. Meyer, "Development of flexible stimulation devices for a retina Implant system," *Proceedings of the 19th Annual International Conference of the IEEE*, vol. 5, pp. 2307–2310, 1997.

[12] D. C. Rodger, W. Li, H. Ameri, S. Saati, P. Menon, E. Meng, J. D. Weiland, M. S. Humayun, and Y.-C. Tai, "Dual-Metal-Layer Parylene-Based Flexible Electrode Arrays for Intraocular Retinal Prostheses," *Invest. Ophthalmol. Vis. Sci.*, vol. 48, no. 5, p. S657, 2007.

[13] D. B. Shire, M. Gingerich, J. F. Rizzo, and J. L. Wyatt, "Recent Developments in Inflatable Prostheses for Epiretinal Stimulation and/or Recording," *Invest. Ophthalmol. Vis. Sci.*, vol. 46, no. 5, p. S1146, 2005.

DOI: 10.1587/elex.5.574
Received June 23, 2008
Accepted July 10, 2008
Published August 10, 2008

ELectronics EXpress

IEICE Electronics Express, Vol.5, No.15, 574–580

1 Introduction

Recently, research both in Japan and overseas has accelerated in the field of artificial sight for patients with acquired sight disabilities; these efforts have concentrated on electrically stimulating the patient's remaining visual nervous system to transmit information to his visual center [1, 2, 3]. Our research group has been developing a system that uses suprachoroidal transretinal stimulation (STS) for this purpose [4]. Cochlear implants share many technical commonalities with visual prostheses, including signal transfer and wireless communication. One research group is actually pursuing development of an artificial vision system in collaboration with a cochlear implant manufacturer [1, 5, 6]. However, there is the technical challenge of establishing an electric connection over the considerable distance from the interiors of the eyeballs to the stimulator unit implanted behind the ears without any cable interruptions due to eye movement. The larger the number of electrodes, the more difficult this becomes. Simulations of artificial vision systems have suggested that over 100 electrodes are necessary to permit activities of daily living (ADL) such as face recognition and walking [7, 8]. One procedure that has been proposed to solve this problem involves combining the stimulating electrode and a miniaturized electronic circuit into a single unit [9]. Another method is to use a multiplexer; this would allow a low number of wires to be used until just before connecting to the stimulating electrodes.

This report proposes an artificial sight system that includes the best features of the cochlear implant, but incorporates a multiplexer that is separate from the hermetically sealed stimulation unit, thus permitting a large number of stimulating electrodes to be used. An implantable wireless power supply and transmitting device were also constructed. Validation tests results and

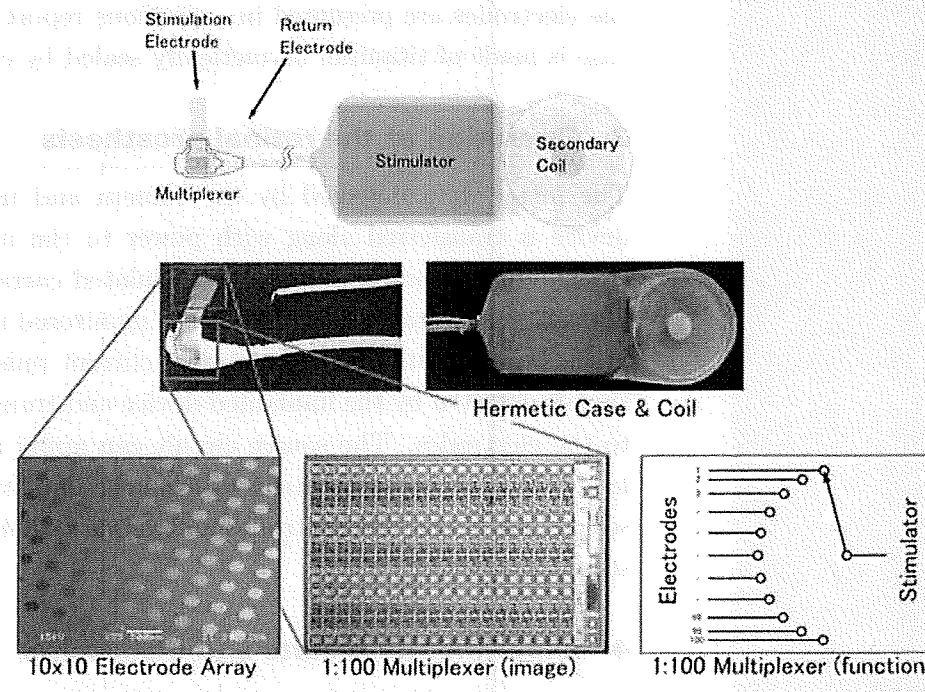

Fig. 1. overview of retina prosthesis.

DOI: 10.1587/elex.5.574
Received June 23, 2008
Accepted July 10, 2008
Published August 10, 2008

directions for future research efforts are discussed.

2 Design of a retinal prosthesis with 100 stimulation electrodes

An artificial vision system consists of both implanted and external components. Figure 1 shows a diagram of the implanted device; it consists of a secondary coil, a stimulator in a hermetically sealed case, a multiplexer, and stimulating and return electrodes. Just as in a cochlear implant, the stimulation unit is implanted behind the ear. The stimulating electrodes and multiplexer are placed on the sclera. The stimulator and multiplexer are connected via a cable composed of six wires which provide power for the multiplexer, the selection signal for the electrode, and the stimulator pulses. Each of the conductors is a stainless steel seven-stranded wire covered with a Teflon insulator. The six conductors and each stimulating electrode are connected with the input/output pads of the multiplexer. A custom integrated circuit (IC) was designed as a multiplexer and is mounted in a flip chip format directly on the board for the stimulating electrodes, with gold bump connections. This chip has dimensions of $4.9 \times 3.2 \times 0.57$ mm (thickness) and was manufactured in a 2 poly-2 metal high-voltage complementary metal oxide semiconductor (CMOS) process. Except for the stimulating electrodes and cables, the entire device is double-coated with $1\,\mu$m of parylene N and $5\,\mu$m of parylene C. The multiplexer is also then coated with silicone molded into a curve that fits the eyeball.

The stimulating electrodes consist of one layer each of gold and platinum on a polyimide base in the form of a 10×10 array of bumps, $200\,\mu$m in diameter, and $30\,\mu$m high. The outermost face of the array is coated with parylene C with just the tips of bumps exposed. More complete details about the electrodes are presented in a previous report [10]. The stimulation unit case is made of titanium hermetically sealed by electron beam welding.

3 Operation of the retinal prosthesis

The image data detected by the camera and transmitted to the external device is transferred along with power to the implanted device. Wireless transmission is on an amplitude-modulated carrier frequency of 16.64 MHz. The internal voltage of the implant is monitored regularly by back-telemetry of the load modulation. Stimulating current pulses are generated using the signals detected by the implanted device and transmitted via the multiplexer to the electrodes. The source circuit can apply a maximum of 10 V to the load. On the basis of instructions from the implanted device, the multiplexer selects one of the 100 electrodes and connects it to the current source in the stimulation unit.

4 Experimental results and discussion

First, in order to verify that the current required by the external device was being output from the designated electrode, a probe was directly attached

DOI: 10.1587/elex.5.574
Received June 23, 2008
Accepted July 10, 2008
Published August 10, 2008